Published in final edited form as:

J Immunol. 2015 November 15; 195(10): 4583–4594. doi:10.4049/jimmunol.1500314.

Sensor Function for Butyrophilin 3A1 in Prenyl Pyrophosphate Stimulation of Human Vγ2Vδ2 T Cells

Hong Wang[*,†] and **Craig T. Morita**[*,†,‡]

[*]Division of Immunology, Department of Internal Medicine, University of Iowa Carver College of Medicine, Iowa City, IA 52242

[†]Department of Veterans Affairs, Iowa City Health Care System, Iowa City, IA 52246

[‡]Interdisciplinary Graduate Program in Immunology, University of Iowa Carver College of Medicine, Iowa City, IA 52242

Abstract

Vγ2Vδ2 T cells play important roles in human immunity to pathogens and in cancer immunotherapy by responding to isoprenoid metabolites, such as (*E*)-4-hydroxy-3-methyl-but-2-enyl pyrophosphate and isopentenyl pyrophosphate. The Ig superfamily protein butyrophilin (BTN)3A1 was shown to be required for prenyl pyrophosphate stimulation. We proposed that the intracellular B30.2 domain of BTN3A1 binds prenyl pyrophosphates, resulting in a change in the extracellular BTN3A1 dimer that is detected by Vγ2Vδ2 TCRs. Such B30.2 binding was demonstrated recently. However, other investigators reported that the extracellular BTN3A1 IgV domain binds prenyl pyrophosphates, leading to the proposal that the Vγ2Vδ2 TCR recognizes the complex. To distinguish between these mechanisms, we mutagenized residues in the two binding sites and tested the mutant BTN3A1 proteins for their ability to mediate prenyl pyrophosphate stimulation of Vγ2Vδ2 T cells to proliferate and secrete TNF-α. Mutagenesis of residues in the IgV site had no effect on Vγ2Vδ2 T cell proliferation or secretion of TNF-α. In contrast, mutagenesis of residues within the basic pocket and surrounding V regions of the B30.2 domain abrogated prenyl pyrophosphate-induced proliferation. Mutations of residues making hydrogen bonds to the pyrophosphate moiety also abrogated TNF-α secretion, as did mutation of aromatic residues making contact with the alkenyl chain. Some mutations further from the B30.2 binding site also diminished stimulation, suggesting that the B30.2 domain may interact with a second protein. These findings support intracellular sensing of prenyl pyrophosphates by BTN3A1 rather than extracellular presentation.

Keywords

human; gamma delta T cell; VγVδT cells; butyrophilin 3A1; prenyl pyrophosphates; isopentenyl pyrophosphate; antigen presentation; isoprenoid metabolism

Address correspondence and reprint requests to Craig T. Morita, M.D., Ph.D., Division of Immunology, Department of Internal Medicine, University of Iowa, Iowa City Veterans Affairs Health Care System, 601 Highway 6 West, Research (151), Iowa City, IA 52246. Craig-Morita@uiowa.edu, Phone (319) 338-0581 Ext. 7608; Fax (319) 339-7162.

Disclosures

C.T.M. is a co-inventor of US Patent 8,012,466 on the development of live bacterial vaccines for activating γδ T cells. H.W. declares no financial or commercial conflict of interest.

Introduction

T cells expressing γδ TCRs have unique roles that bridge innate and adaptive immunity. However, relatively few Ags have been identified for these cells, and the mechanisms by which they detect alterations in cells due to stress, tissue damage, or infection have not been defined. The major subset of human γδ T cells expresses Vγ2Vδ2 TCRs (also termed Vγ9Vδ2 TCRs) (1). These cells use their TCRs to detect alterations in isoprenoid metabolism by responding to prenyl pyrophosphate metabolites (2). Vγ2Vδ2 T cells are preferentially stimulated by the foreign microbial isoprenoid metabolite, (*E*)-4-hydroxy-3-methyl-but-2-enyl pyrophosphate (diphosphate) (HMBPP) that is produced in the 2-*C*-methyl-D-erythritol-4-phosphate pathway used by many eubacteria and all apicomplexan parasites (3, 4). Vγ2Vδ2 T cells are also stimulated by the self-metabolite, isopentenyl pyrophosphate (diphosphate) (IPP), which is produced in the mevalonate pathway (5).

Vγ2Vδ2 T cells play important roles in microbial immunity (reviewed in Ref. 1). A number of different microbial infections expand Vγ2Vδ2 T cells to up to 50% or more of circulating T cells. These cells can traffic to peripheral sites where they secrete Th1 cytokines such as IFN-γ and TNF-α, inflammatory chemokines, and growth factors while killing infected cells. Released bacteria and parasites can then be killed by granulolysin (6) and antimicrobial peptides (7, 8).

Vγ2Vδ2 T cells can also mediate tumor immunity. Activated Vγ2Vδ2 T cells can use their TCR and NK receptors to recognize and kill a variety of tumor cells, irrespective of their tissue origin, MHC expression, or MHC-haplotype (reviewed in Ref. 1). The aminobisphosphonate, zoledronate, has been used to expand Vγ2Vδ2 T cells for adoptive cancer immunotherapy. Aminobisphosphonates (9) and alkylamines (10) expand Vγ2Vδ2 T cells by inhibiting farnesyl pyrophosphate synthase, resulting in the accumulation of the upstream IPP metabolite that stimulates the Vγ2Vδ2 T cells (11–13). In clinical trials, vaccines stimulating Vγ2Vδ2 T cells (bromohydrin pyrophosphate or aminobisphosphonates), in conjunction with low-dose IL-2, resulted in partial remissions for some patients with lymphoma (14) and stabilized disease in patients with metastatic prostate cancer (15) and lung cancer (16) without major toxicities or autoimmunity. Adoptive transfer of Vγ2Vδ2 T cells in conjunction with i.v. zoledronate resulted in a durable complete remission in one patient with metastatic renal cell carcinoma (17) and slowed disease in other patients with renal cell carcinoma (18). Patients with other tumor types also showed responses when given concurrently with other therapies (19).

Despite the importance of Vγ2Vδ2 T cells in human immunity, relatively little had been known about how prenyl pyrophosphates stimulate them. Recently, however, the butyrophilin (BTN)3A1 Ig superfamily protein was shown to be required for this stimulation (20–23). We (22) and others (21) did not find any evidence to support a costimulatory role for BTN3A1. BTN3A1 also does not stimulate indirectly by altering isoprenoid metabolism (21, 22). Moreover, because BTN3A1 stimulation is mediated through the Vγ2Vδ2 TCR (21, 22), all evidence points to a direct role for BTN3A1 in prenyl pyrophosphate stimulation. However, the mechanism by which BTN3A1 functions is controversial. Results

from one study (23) support a mechanism wherein BTN3A1 functions as an Ag-presenting molecule by binding prenyl pyrophosphates in a shallow basic pocket on its extracellular IgV domain. The prenyl pyrophosphate-BTN3A1 complex is then hypothesized to be recognized by the Vγ2Vδ2 TCR for γδ T cell activation (23, 24), much as αβ TCRs recognize peptide-MHC class I or II complexes or lipid-CD1 complexes.

In contrast, results of our studies (22), as well as those of Sandstrom et al. (25) and other investigators (21, 26, 27), suggest that BTN3A1 binds prenyl pyrophosphates through its intracellular B30.2 domain. A structural model of the BTN3A1 B30.2 domain predicts a basic pocket on its binding face not found on other non-butyrophilin B30.2 domains (22). Basic residues are commonly found in binding sites for phosphates because their positively charged amino groups can form hydrogen bonds to the negatively charged phosphate moieties. Based on the presence of this basic pocket in the BTN3A1 B30.2 domain, the evidence that this domain is required for BTN3A1 function (21), and the lack of high-affinity binding of a prenyl pyrophosphate photoaffinity compound to the extracellular domains of BTN3A1 or BTN3A2, we proposed that prenyl pyrophosphates bind to the basic pocket on the intracellular B30.2 domain of BTN3A1, perhaps in association with a second protein (28). Recent determination of the structure of the BTN3A1 B30.2 domain and in vitro binding studies by the Adams laboratory (25) and other investigators (26, 27) support this model. This binding would then cause changes in the conformation and/or distribution of the extracellular BTN3A1 dimers that are detected by the Vγ2Vδ2 TCR. Thus, BTN3A1 would function as a sensor for intracellular isoprenoid metabolism to signal changes to Vγ2Vδ2 T cells.

In this study, we sought to distinguish between these two mechanisms of action by mutating amino acid residues in the IgV and B30.2 binding sites and testing the mutant proteins functionally for their ability to support HMBPP stimulation of Vγ2Vδ2 T cells.

Materials and Methods

Mutagenesis of BTN3A1 cDNA

The pCMV6-Entry expression plasmid for BTN3A1 (transcript variant 1, True ORF Gold) was purchased from OriGene Technologies (Rockville, MD). Mutations in the IgV binding site were selected based on the IgV:HMBPP crystal structure (23). Mutations in the binding face of the B30.2 domain of BTN3A1 were selected on the basis of our model of the B30.2 domain (22). The primers used to generate mutations in the BTN3A1 cDNA were designed using the Primer Design program (http://www.genomics.agilent.com/primerDesignProgram.jsp; Agilent Technologies, Santa Clara, CA) and synthesized by Integrated DNA Technologies (Coralville, IA). The mutations in BTN3A1 were created by PCR using the primers and the QuikChange II Site-Directed Mutagenesis kit (Agilent Technologies). Expression plasmids containing mutated BTN3A1 cDNAs were purified using the QIAprep Spin Miniprep kit (QIAGEN, Valencia, CA) and the cDNAs were sequenced to confirm the presence of the mutations and to ensure that no other mutations were introduced.

Transfection of small interfering RNAs and cDNAs

Silencer-27 small interfering RNAs (siRNAs) for BTN3A1 and control duplexes were purchased from OriGene and resuspended in the provided duplex buffer to obtain a 20 μM stock solution. The stock solution was further diluted to 5 μM with the same buffer for transfection or cotransfection with cDNA. For transfections, HeLa cells were plated at 1.7×10^5 cells/well in six-well plates 1 d prior to transfection. To transfect a well of HeLa cells with siRNA, 4 μl of a control siRNA or BTN3A1 siRNA oligo A was added to 100 μl of Opti-MEM I medium (Life Technologies, Grand Island, NY) and then mixed by vortexing. To transfect with cDNA, 100 ng of a control plasmid or the BTN3A1 expression plasmid was added to 100 μl of Opti-MEM I medium and then mixed by flicking. For cotransfection of BTN3A1 siRNA oligo A and BTN3A1 cDNA, 100 ng of cDNA was added to 100 μl of Opti-MEM I medium followed by 4 μl of siRNA and mixing. Then, 4.5 μl of Attractene transfection reagent (QIAGEN) was added to the siRNA and/or cDNA preparation, vortexed for 5 s, incubated at room temperature for 15 min, and added dropwise to a well of HeLa cells. Media was replaced at 6, 24, and 48 h. After 72 h, the transfectants were trypsinized and harvested for analysis by flow cytometry and for use in T cell assays. Note that the BTN3A1 siRNA oligo A is specific for a sequence in the 3' untranslated region of BTN3A1 that is not present in the BTN3A1 cDNA expression plasmid. Therefore, siRNA treatment only suppresses endogenous BTN3A1 mRNA.

mAbs and flow cytometry

To assess BTN3 expression, cells were stained with PE-conjugated anti-BTN3/CD277 (20.1, also termed BT3.1) (BioLegend, San Diego, CA) or with an isotype control PE-P3 mAb (eBioscience, San Diego, CA) on ice for 2 h, washed, and analyzed by flow cytometry (22).

T cell proliferation and cytokine secretion assays

The Vγ2Vδ2 CD8αα$^+$ 12G12 T cell clone was maintained by periodic restimulation with PHA. T cell-proliferation assays were performed as described previously (22). Assays for prenyl pyrophosphate (HMBPP) and PHA stimulation were done in singlet or duplicate using round-bottom 96-well plates using $0.5–1.0 \times 10^5$ 12G12 T cells/well with 1.0×10^5 mitomycin C-treated HeLa APCs/well. Stimulating compounds were tested at one-half log dilutions, as indicated in the figure legends. Because there were differences in the maximal proliferation of Vγ2Vδ2 T cells stimulated by different HeLa transfectants, the data was normalized by setting the plateau proliferation values for HMBPP as 100% or, in cases where HMBPP proliferation did not reach plateau levels, using the HMBPP plateau values for control siRNA treated cells. To assess TNF-α responses, culture supernatants were harvested after 16 h and assayed for TNF-α levels by DuoSet sandwich ELISA (R&D Systems, Minneapolis, MN).

Human BTN3A1 structures

BTN3A1 structures presented in this article were the BTN3A1 extracellular domains (PDB 4F80) (20), the BTN3A1 IgV domain complexed with HMBPP (PDB 4K55) or IPP (PDB 4JKW) (23), and the BTN3A1 B30.2 domain with (PDB 4N7U) and without (PDB 4N7I) (*E*)-1-hydroxy-2-methyl-pent-2-enyl pyrophosphonate (HMBcPP) (25). The IgV:IgC

homodimer structure of BTN3A1 was provided by Dr. Erin Adams (University of Chicago). Residue numbering starts with residue 31, as used by Sandstrom et al. (25). To directly compare with other BTN3A1 extracellular domain structures, subtract one from the numbering used by Palakodeti et al. (20) and subtract three from the numbering used by Vavassori et al. (23). Modeling of the BTN3A1 B30.2 domains was done at the Swiss-Model Web site (http://swissmodel.expasy.org/) using standard settings and was based on the structure of pyrin/TRIM20 (PDB 2Wl1). The coiled coil domain of BTN3A1 is predicted to be from residue 242 to 282 (coiled coil structure probability >18%) using the MARCOIL program (29) (http://toolkit.tuebingen.mpg.de/marcoil). A model of this region was made using the CCBuilder program (30) (http://coiledcoils.chm.bris.ac.uk/app/cc_builder/) under standard settings, assuming a parallel homodimeric structure and using BTN3A1 residues 240–282. The BTN3A1 structural model is composed of the crystal structure of the BTN3A1 extracellular homodimer (PDB 4F80), the transmembrane domain from the DAP12 homodimer (PDB 2L34) (31), the model of the coiled coil BTN3A1 homodimer (residues 242–282), and the crystal structure of the B30.2 domain homodimer from BTN3A1 (PDB 4N7I). The amino acid linking segment from residues 283–297 is not shown. All figures were produced using PyMOL X11 Hybrid version 1.5.0.4 (Schrödinger, LLC, New York City, NY). The BTN3A1 domains are identically scaled using a PyMOL script. *In silico* mutations were made in PyMOL using Mutagenesis Wizard. Electrostatic surface potential was calculated by the APBS 1.3 PyMOL plugin (32) with internally generated PQR files for the extracellular domains and with externally generated PQR files from the PDB2PQR website (http://nbcr-222.ucsd.edu/pdb2pqr_1.8/) using the PARSE forcefield for the B30.2 domain and the AMBER forcefield for the coiled coil domain. Surface potentials are colored from red (negative potential, −10 kT) to blue (positive potential, +10 kT).

Results

Structure of BTN3A1 molecules

Like B7 and PD-L proteins, BTN3A1 is an Ig superfamily protein with IgV and IgC extracellular domains. BTN3A1 is expressed on the surface of all human cells as a V-shaped homodimer that forms through the interaction of IgC residues (20). BTN3A1 differs from B-7 and PD-L proteins by the presence of an intracellular B30.2 domain (also termed a PRYSPRY domain) that is predicted to be connected to the transmembrane region by a coiled coil domain (Fig. 1A). The two other family members, BTN3A2 and BTN3A3, have highly homologous IgV domains to BTN3A1 (100% and 99% amino acid identity, respectively) and slightly less homologous IgC domains (91% and 90%) but differ at their coiled coil domains (34% and 48%) and intracellular tails with BTN3A2 lacking a B30.2 domain and BTN3A3 having a B30.2 domain that shares 86% amino acid identity to that of BTN3A1. A composite model of the full-length BTN3A1 protein (Fig. 1B) shows the extracellular V-shaped IgV:IgC homodimer, the transmembrane regions, the stalk-like coiled coil domain, and the intracellular B30.2 domains. Based on binding and structural studies, a binding site for prenyl pyrophosphates has been proposed in a shallow basic region on the outer face of the IgV domain (Fig. 1B) (23). However, binding and structural studies have

also demonstrated prenyl pyrophosphate binding to a strongly basic pocket in the center of the binding face of the B30.2 domain (Fig. 1B) (25, 26).

Mutation of amino acid residues making up the proposed BTN3A1 IgV binding site for prenyl pyrophosphates has no effect on HMBPP stimulation of Vγ2Vδ2 T cells

The IgV binding site for prenyl pyrophosphates has equilibrium binding constants (K_d) for IPP and HMBPP of 69.9×10^{-6} M and 3.1×10^{-6} M, respectively (23). Structural studies of the BTN3A1 IgV domain in complex with IPP or HMBPP showed their binding to a shallow basic groove located on the side of the IgV domain. The extracellular portion of BTN3A1 was also shown to directly interact with multimeric Vγ2Vδ2 TCRs, with IPP facilitating this interaction (23). Taken together, these findings led some investigators to conclude that BTN3A1 functions as a prenyl pyrophosphate-presenting molecule for Vγ2Vδ2 T cell recognition (23, 24, 33). However, the interpretation of the BTN3A1-IPP/HMBPP structural data has been disputed (25). Moreover, the binding of prenyl pyrophosphates to the IgV domain of BTN3A1 is significantly weaker than the binding of peptides to MHC class I and class II molecules (whose binding constants range between 10^{-7} M to 10^{-9} M). To functionally assess the importance of the IgV binding site in the stimulation of Vγ2Vδ2 T cells, we mutated each of the amino acid residues reported to make contact with the prenyl pyrophosphates to alanine (or to glutamic acid for one tyrosine residue). Each mutant BTN3A1 protein was then expressed in HeLa cells whose endogenous BTN3A1 was inhibited by an siRNA specific for the 3' untranslated region of BTN3A1 mRNA that is lacking in the transfected BTN3A1 mRNA. The cotransfected HeLa cells were then used as presenting cells for HMBPP and mitogen (PHA) stimulation of Vγ2Vδ2 T cells.

The addition of untransfected HeLa cells increased the magnitude of the proliferative response of 12G12 Vγ2Vδ2 T cells to varying degrees, but it did not alter their sensitivity to HMBPP stimulation (EC_{50} of 0.38 nM for T cells alone versus 0.64 nM with HeLa cells), whereas Va2 tumor cells increased both the magnitude and sensitivity of 12G12 T cells to HMBPP (EC_{50} was 0.07 nM with Va2 cells) (Supplemental Fig. 1). The addition of HeLa cells transfected with control siRNA or a control expression plasmid similarly did not affect the sensitivity of 12G12 T cells to HMBPP (Supplemental Fig. 2B, 2C). In contrast, BTN3A1 siRNA-treated HeLa cells decreased the sensitivity of 12G12 T cells to HMBPP stimulation an average of 33-fold (16.6-fold to 68.4-fold), increasing the EC_{50} to between 3 and 100 nM compared with HeLa cells that had been treated with BTN3A1 siRNA and transfected with a BTN3A1 cDNA expression plasmid (Supplemental Fig. 2A–C). Therefore, this assay was used evaluate the function of BTN3A1 in prenyl pyrophosphate stimulation.

Consistent with our previous study (22), siRNA directed against the 3' untranslated region of BTN3A1 mRNA selectively decreased endogenous BTN3A1 expression (Fig. 2, *bottom left panel*). In this experiment, untreated HeLa cells stimulated half-maximal proliferation (EC_{50}) of the 12G12 Vγ2Vδ2 T cell clone at 2 nM whereas HeLa cells treated with siRNA specific for BTN3A1 required 30 nM HMBPP, a 15-fold shift in the dose-response curve (Fig. 2, *bottom panels*). Cotransfection with a plasmid expressing wild-type BTN3A1 restored BTN3A1 expression to levels 3.9-fold higher than that of untreated cells (Fig. 2, *left*

panels). Higher expression of BTN3A1 improved the ability of the HeLa cells to stimulate Vγ2Vδ2 T cells by 2.9-fold (EC_{50} decreased from 2 nM to 0.7 nM for proliferative responses and from 13 nM to 6 nM for TNF-α responses) (Fig. 2, panels labeled wild-type BTN3A1), indicating that the endogenous level of BTN3A1 is suboptimal in HeLa cells. These results are consistent with our previous study (22) in which siRNA inhibition of BTN3A1 in HeLa accessory cells resulted in a 6.7-fold increase in EC_{50} with IPP stimulation of 12G12 Vγ2Vδ2 T cells, whereas overexpression of wild-type BTN3A1 improved the ability of HeLa cells to stimulate by decreasing the EC_{50} 3.9-fold. Increasing BTN3A1 expression on other tumor cells also enhanced their ability to support HMBPP stimulation of Vγ2Vδ2 T cells (23).

Using this cotransfection method, we tested BTN3A1 proteins that had mutations in the IgV binding site. Mutation of residues in the site had no effect on the expression levels of the mutant BTN3A1 proteins (Fig. 2, *left panels*). Importantly, there were no differences in the ability of the mutant BTN3A1 proteins to stimulate the proliferation of Vγ2Vδ2 T cells in response to HMBPP. The EC_{50} values for the BTN3A1 mutants (0.65–0.73 nM) were identical to that of wild-type BTN3A1 (0.70 nM) (Fig. 2, *middle panels*). Similar results were obtained when measuring TNF-α secretion by 12G12 Vγ2Vδ2 T cells. Although higher HMBPP concentrations were required for half-maximal TNF-α secretion (6.0 nM for TNF-α secretion versus 0.7 nM for proliferation), there were no significant differences in the EC_{50} between the various mutant and wild-type BTN3A1 proteins with regard to TNF-α secretion (Fig. 2, *right panels*). Additionally, expression of the mutated BTN3A1 proteins did not alter the ability of transfected HeLa cells to support PHA mitogen stimulation of Vγ2Vδ2 T cells, arguing against unexpected effects of transfection on the HeLa cells (Fig. 2, *middle* and *right panels*).

Two structures were reported for the IgV domain that differ slightly in the positions of the amino acid side chains [Fig. 3, structures in the *top* and *middle panels* are from Palakodeti et al. (20) and structures in the *bottom panels* are from Vavassori et al. (23)]. The location of each mutated residue in the IgV binding site is shown as a colored surface (Fig. 3, *top right* and *bottom left panels*). The putative prenyl pyrophosphate binding site corresponds to a basic groove on the outer side of the IgV domain (blue region in Fig. 3, *top left panel*) that is near the binding site of the stimulatory 20.1 mAb (20–22). The prenyl pyrophosphate binding site (Fig. 3, *bottom left panel*) is centered on the Lys^{36} basic residue, with the negatively charged pyrophosphate moiety making electrostatic and hydrogen bonds to four charged or polar amino acids (Asp^{34}, Lys^{36}, Arg^{58}, and Gln^{99}) and hydrophobic interactions with two tyrosine residues (Tyr^{97} and Tyr^{104}). *In silico* modeling of the mutation of Lys^{36} to alanine (Fig. 3, *middle left panel*) and Arg^{59} to alanine (Fig. 3, *middle right panel*) predicts decreases in the surface potential as well as alterations in the shape of the binding site for each mutation. Despite the predicted effects of the alanine mutations, mutant BTN3A1 proteins with these and other mutations in the binding site showed no functional differences from wild-type BTN3A1 upon HMBPP stimulation of Vγ2Vδ2 T cells (Fig. 2) with regard to proliferation or TNF-α secretion. Mutation of one of the tyrosines to glutamic acid (Tyr97Glu) that would disrupt hydrophobic interactions with the alkenyl chain of HMBPP also had no effect on HMBPP stimulation (Fig. 3). Thus, our data does not support a role for the IgV binding site in HMBPP stimulation of Vγ2Vδ2 T cells.

BTN3A1 function in HMBPP stimulation of Vγ2Vδ2 T cells is critically dependent on residues involved in prenyl pyrophosphate binding to the B30.2 domain

We next assessed the effect of alanine mutations in the intracellular B30.2 domain. Our structural model predicts a basic pocket in the center of the B30.2 binding face that we hypothesized could function in prenyl pyrophosphate recognition (22). The model was used to guide selection of potentially critical residues in the B30.2 domain for mutagenesis. The recent BTN3A1 B30.2 crystal structure reported by Sandstrom et al. differs from the model by 0.958 $Å^2$ root mean square deviation and confirms the presence of the basic pocket with binding of a HMBPP analog (25).

The basic pocket and surrounding loops are on one face of the B30.2/PRYSPRY domain. This face has been found to interact with other proteins in cases where B30.2 binding has been defined structurally or through the loss of function due to mutation (34–38). The loops of the B30.2 domain have been divided into four variable (V) regions. In tripartite motif-containing (TRIM) 5α proteins these V regions make contact to retroviral capsids (39), whereas TRIM21 V regions make contact to Ig Fc regions (35). To assess the functional importance of the B30.2 domain of BTN3A1, residues in the basic pocket and surrounding V regions were mutated to alanine, and the resulting mutant proteins were tested for their ability to stimulate Vγ2Vδ2 T cells.

Within the basic pocket, alanine substitution of each of the arginine residues (Arg412Ala, Arg418Ala, and Arg469Ala) that make hydrogen bonds to the HMBPP analog, HMBcPP (25), completely abolished HMBPP stimulation of Vγ2Vδ2 T cell proliferation but only Arg412Ala and Arg469Ala completely abolished HMBPP-induced TNF-α secretion (Fig. 4, V3 region and Basic Pocket). Mutation of lysine 393 (Lys393Ala) (Fig. 5, V2 region), which also makes a hydrogen bond to the pyrophosphate moiety similarly abolished HBMPP stimulation of proliferation and TNF-α secretion. These results show that mutation of the four proposed contact residues diminish or abrogate proliferation and TNF-α secretion by Vγ2Vδ2 T cells. Histidine 351 is normally buried and makes no contacts with HMBcPP. However, the presence of arginine instead of histidine at this position in the B30.2 domain of BTN3A3 prevents BTN3A3 from stimulating Vγ2Vδ2 T cells (25). BTN3A1 exhibited a similar loss of function with the mutation of histidine 351 to alanine (His351Ala) because this mutation decreased Vγ2Vδ2 T cell proliferation and TNF-α secretion to background levels (Fig. 4, Basic Pocket). These finding extend the results of Sandstrom et al. (25), who found that concurrent charge-reversal mutation of all five residues abrogated function as well as in vitro binding to HMBcPP. Thus, all of the B30.2 residues that make hydrogen bonds to HMBcPP are essential for HMBPP stimulation of Vγ2Vδ2 T cells. Moreover, the loss of hydrogen bonding by any single residue (except for Arg^{418}) is capable of causing the complete loss of BTN3A1 function.

Other B30.2 residues surrounding the basic pocket were also required for HMBPP stimulation of Vγ2Vδ2 T cells. Mutation of the acidic residue, E376, in the V4 region at the edge of the basic pocket also abolished stimulation of proliferation and TNF-α secretion by Vγ2Vδ2 T cells (Fig. 4, V4 region). Similarly, mutation of aromatic residues Trp^{350} and Tyr^{352} in the V1 region and Trp^{391} in the V2 region (Fig. 5, V1 and V2 regions) also abolished or decreased stimulation. The Trp^{350} and Trp^{391} residues likely facilitate binding

of the carbon chain of prenyl pyrophosphates; however, given that they lie on the extreme edge of the binding site, they could potentially interact with a second protein. Lysine 389, which lies adjacent to these residues but on the side of the B30.2 domain, also might interact with a second protein given that mutation of this residue partially decreased prenyl pyrophosphate stimulation of Vγ2Vδ2 T cell proliferation (EC_{50} increased 5.3-fold) and TNF-α secretion (EC_{50} increased 6.3-fold) (Fig. 5, V2 region).

Other amino acid residues located further from the binding site of the B30.2 domain were not critical for HMBPP stimulation of Vγ2Vδ2 T cells. Mutation of charged and polar residues in the V1, V3, and V4 regions on the distal edges or sides of the binding face did not affect HMBPP stimulation (Fig. 4, 5, V1, V3, and V4 regions).

The locations of essential residues on the B30.2 crystal structure clearly encompass the prenyl pyrophosphate binding site (Fig. 6C–E). As noted above, the B30.2 domain of BTN3A1 can be divided into four V regions (Fig. 6A) surrounding a central basic pocket (Fig. 6B). Mutations made in the B30.2 domain (Fig. 6C) that abrogate or diminish HMBPP stimulation of Vγ2Vδ2 T cells for proliferation (Fig. 6D, *left panel*) or TNF-α secretion (Fig. 6D, *right panel*) surround and include the central basic pocket where HMBcPP binds. The location of these mutations and their effect on Vγ2Vδ2 T cell proliferation in relation to bound HMBcPP are shown in Fig. 6E. Mutation of B30.2 residues that make hydrogen bonds to the pyrophosphate moiety abrogate or greatly diminish proliferation and TNF-α secretion by Vγ2Vδ2 T cells. Thus, our results demonstrate that the B30.2 binding site is essential for Vγ2Vδ2 T cell stimulation by prenyl pyrophosphates (model 2, Fig. 7) whereas the extracellular IgV binding site is not (model 1, Fig. 7).

Discussion

The results in this study provide evidence that BTN3A1 acts as a sensor for intracellular isoprenoid metabolism rather than as an Ag-presenting molecule. Mutation of residues in the proposed IgV binding site had no effect on prenyl pyrophosphate stimulation of Vγ2Vδ2 T cells, whereas mutation of residues within or closely surrounding the B30.2 binding site completely abrogated stimulation. The lack of functional effects of mutations in the IgV site is consistent with the assertion that a polyethylene glycol molecule rather than a prenyl pyrophosphate is bound to this site in the crystal structure (25). Also, there are no other potential binding sites for prenyl pyrophosphates in the BTN3A1 extracellular domain other than the one mutated in this study (20, 23). Thus, there is no evidence for a presentation function for BTN3A1 (model 1, Fig. 7). Instead, our functional results coupled with the B30.2 crystal structure, functional studies, and in vitro binding studies reported by Sandstrom et al. (25) and Rhodes et al. (27) strongly support a sensor function for the B30.2 domain of BTN3A1 (model 2, Fig. 7).

B30.2 domains and the evolutionarily older PRYSPRY domains (40) are common protein-interaction structures found in 97 human proteins (41) and 77 murine proteins (42). These include other butyrophilin proteins, negative regulators of the JAK/STAT pathway (SOCS proteins), a subset of the tripartite motif (TRIM) E3 ligase proteins (43, 44), and others (40, 41). Many of the proteins are involved in innate immunity (40, 44).

All B30.2 domains share a conserved domain architecture consisting of two antiparallel β-sheets with six extended, highly diverse loops that are similar to Ig CDR regions (35). Where ligand binding to B30.2 domains has been defined by either crystal structures or nonfunctional mutants (34–39, 45), interactions have mapped to the face of the B30.2 domain where these hypervariable loops lie. Although the exact binding sites on this face vary, many involve the central region of the domain (35, 37, 41). In other B30.2 domains where crystal structures are available, this central region has a neutral surface potential (22). However, the crystal structure of the B30.2 domain of BTN3A1 and models of the B30.2 domains of BTN3A3, BTNL3, BTNL8, and BTNL9 have deep central pockets with strongly basic surface potentials on the canonical binding face (22, 25).

The basic pocket of the B30.2 domain of BTN3A1 was identified as the binding site for prenyl pyrophosphates by the binding of HMBcPP to a cross-linked crystal of apo B30.2 (25). In this article, we show that mutation of residues in the B30.2 domain (Arg^{412}, Arg^{418}, Arg^{469}, and Lys^{393}) that directly form hydrogen bonds to the pyrophosphate moiety, diminish or abrogate HMBPP stimulation of Vγ2Vδ2 T cells for proliferation and TNF-α secretion (Fig. 6D, E). The loss of hydrogen bonding by any single residue (except for Arg^{418}) resulted in the complete loss of BTN3A1 function in HMBPP stimulation of Vγ2Vδ2 T cells. In addition to these basic residues, aromatic residues on the distal end of the central pocket (Tyr^{352}, Trp^{350}, Trp^{391}) where the alkenyl chain is positioned also were essential for BTN3A1 stimulation. However, residues located further from the central pocket were not (Fig. 6D). Thus, our mutational analysis clearly demonstrates the importance of the central binding pocket and surrounding regions of the B30.2 domain in determining the BTN3A1 function in prenyl pyrophosphate stimulation of Vγ2Vδ2 T cells.

The primary exception is residue Lys^{389} which is located on the side of the B30.2 domain. The K389A mutant BTN3A1 protein reduced, but did not completely abrogate, stimulation of Vγ2Vδ2 T cell proliferation and TNF-α secretion (Fig. 5). Although mutation of this residue could alter the conformation of the B30.2 domain, it is also possible that this residue interacts with another intracellular protein. Support for the involvement of a second protein comes from the fact that expression of BTN3A1 in murine or Chinese hamster cells is not sufficient to allow them to support HMBPP stimulation of Vγ2Vδ2 T cells whereas transfer of chromosome 6, which encodes other proteins in addition to BTN3A1, does (23, 28).

One potential limitation of this study is the use of the 12G12 Vγ2Vδ2 T cell clone to determine BTN3A1 functional activity. Clearly, further testing with additional Vγ2Vδ2 clones/lines will be required to determine the impact of differences in the CDR3 regions on stimulation by mutant BTN3A1 molecules. However, we believe that the results obtained in this study will be valid for most Vγ2Vδ2 T cells, because the 12G12 T cell clone is representative of the majority of adult Vγ2Vδ2 T cells that respond to prenyl pyrophosphates. The 12G12 clone was derived by stimulation of PBMCs from a patient with tuberculoid leprosy with a sonicate from *Mycobacterium tuberculosis* H37Ra (46). Similar to most adult Vγ2Vδ2 T cells, the 12G12 clone expresses NKG2D, is cytolytic, and secretes IFN-γ and TNF-α. It also expresses the CD8αα homodimer as do many adult Vγ2Vδ2 T cells. As such, we and our collaborators (5, 10, 13, 22, 46–61) used this clone extensively in our studies on Vγ2Vδ2 T cells as representative of an adult Vγ2Vδ2 T cell.

Importantly, the 12G12 Vγ2Vδ2 TCR has sequence characteristics found in the majority of Vγ2Vδ2 TCRs stimulated by prenyl pyrophosphates (Supplemental Table I) (62). The 12G12 Vγ2 chain uses the Jγ1.2 gene segment (also termed JγP), which is used by the majority of reactive Vγ2Vδ2 TCRs (62–66) and whose frequency is increased further with prenyl pyrophosphate stimulation (63, 64) and decreased with anergy (67). The length of the Vγ2 CDR3γ region is one less than the length most frequently used by reactive Vγ2Vδ2 TCRs, where the CDR3γ length of the majority of reactive Vγ2 chains is within one amino acid (Supplemental Fig. 3) (62, 63, 67). The Vγ2Jγ1.2 sequence has no unusual features and is identical to the Vγ2 chain expressed by the DG.SF13 clone. This TCR was used in our transfection and mutagenesis experiments defining critical residues in the Vγ2Vδ2 TCR that are required for prenyl pyrophosphate stimulation (2, 62, 68).

The 12G12 Vδ2 chain also has sequence characteristics found in reactive Vδ2 chains. It has a leucine residue at position 97 in the CDR3δ region, which is the most commonly used residue in this position for reactive Vγ2Vδ2 TCRs. Although the length of the CDR3δ region is more variable than the Vγ2 CDR3γ region, the length of the 12G12 CDR3δ region is the most frequently represented among reactive Vγ2Vδ2 TCRs (Supplemental Fig. 3). The CDR3δ sequence also has no unusual features compared with other reactive Vγ2Vδ2 TCRs (Supplemental Table I). For these reasons, we believe that the results obtained in this study will be valid for most, if not all, Vγ2Vδ2 T cells.

The addition of HeLa cells lacking BTN3A1 due to siRNA treatment or that expressed nonfunctional mutant BTN3A1 decreased the sensitivity of 12G12 T cells to HMBPP stimulation though T cell-T cell presentation (Supplemental Fig. 2). The mechanism behind this decrease in Vγ2Vδ2 T cell sensitivity is unclear. Although increased degradation of HMBPP via alkaline phosphatase from tumor cells is possible, this should be similar between the different HeLa cell populations. Moreover, we doubt that BTN3A1-specific siRNA released from HeLa transfectants would inhibit BTN3A1 expression by 12G12 T cells rapidly enough to alter the release of TNF-α from preformed stores, as was observed in our experiments. Our working hypothesis is that this decrease in sensitivity is due to interference with T cell-T cell conjugate formation by nonstimulatory APCs that lack BTN3A1 expression or that express nonfunctional mutant BTN3A1 molecules. Supporting this possible mechanism, the addition of murine A20 B cell lymphoma cells or P815 mastocytoma cells also decreased 12G12 T cell sensitivity to HMBPP stimulation (EC_{50} of 7.2 nM and 4.3 nM, respectively, Supplemental Fig. 3D). Moreover, Vγ2Vδ2 T cells were shown to form mature immune synapses with THP-1 myelomonocytic tumor cells for prolonged periods (up to 1 h) in the absence of stimulation with exogenous prenyl pyrophosphates (69). This interaction does not result in cytokine production (or, presumably, proliferation). This differs from the situation with mature αβ T cells that form immune synapses in response to TCR engagement with their respective peptide-MHC complexes (70–72). Taken together, these findings provide evidence that the presence of cells lacking functional BTN3A1, either human or murine, decrease the sensitivity of Vγ2Vδ2 T cells to stimulation by HMBPP and that our assay can be used to identify critical regions in BTN3A1.

If BTN3A1 is functioning as a sensing molecule, how is the binding of prenyl pyrophosphates to the BTN3A1 B30.2 intracellular domains detected by Vγ2Vδ2 T cells at the cell surface? One likely explanation is that the intracellular binding of prenyl pyrophosphates to the B30.2 domain in conjunction with a second protein or proteins, induces a conformational change in the extracellular IgV-IgC dimer through "inside-out" signaling (model 2, Fig. 7). In the stimulatory conformation, BTN3A1 would either bind directly to the Vγ2Vδ2 TCR or to a second protein that would then bind to the Vγ2Vδ2 TCR. Support for this model comes from the action of the 20.1 anti-BTN3 mAb. Binding of the 20.1 mAb to the IgV domain of BTN3A1 activates Vγ2Vδ2 T cells in an identical manner to HMBPP, and this activation is mediated by the Vγ2Vδ2 TCR (21, 22). Moreover, 20.1 mAb binding to the IgV domains of BTN3A2 and BTN3A3 also stimulate Vγ2Vδ2 T cells, despite the lack of a B30.2 domain in BTN3A2 and the presence of an arginine in the 351 position in the B30.2 domain of BTN3A3, instead of the histidine residue found in BTN3A1 that renders BTN3A3 unable to mediate stimulation of Vγ2Vδ2 T cells. Binding of the 20.1 mAb to the IgV domain induces a 19-Å rotational shift in the BTN3A1 dimer (20); perhaps it is this common altered conformation that is detected by the Vγ2Vδ2 TCR. Prenyl pyrophosphate binding to the B30.2 domain could induce a similar rotational shift. As detailed above, this binding process likely requires a second protein encoded on chromosome 6. Prenyl pyrophosphate binding to the BTN3A1 B30.2 domain may cause conformational changes that are transmitted up the coiled coil domain to the extracellular dimer. Supporting this hypothesis, conformational changes in the coiled coil region were noted upon binding of HMBPP to the B30.2 domain when assessed by nuclear magnetic resonance (26), and coiled coil domains were shown to transmit signals from the sensor to the kinase domains of bacterial sensor histidine kinases, potentially though rotary movements or helix destabilization (73).

Monitoring intracellular metabolism through the recognition of a specific conformation of the BTN3A1 extracellular dimer would be an efficient way for Vγ2Vδ2 T cells to detect alterations in intracellular isoprenoid metabolism at the cell surface. The requirement for the Skint1 Ig superfamily protein for the development of murine dendritic epidermal Vγ5Vδ1 T cells (74) is reminiscent of the requirement for BTN3A1 for prenyl pyrophosphate stimulation of Vγ2Vδ2 T cells, especially given that the function of Skint1 is dependent on its intracellular tail (75). Other BTN and BTNL proteins could serve similar functions for other γδ T cell subsets that are responding to other classes of molecules associated with stress or infection. This type of recognition may be a common mechanism used by many γδ T cell subsets and represents a new paradigm for γδ T cell recognition.

Supplementary Material

Refer to Web version on PubMed Central for supplementary material.

Acknowledgments

We thank Zhimei Fang for technical assistance. We thank Mohanad Nada, Yoshimasa Tanaka, and Eric Oldfield for helpful discussion.

This work was supported by Department of Veterans Affairs (Veterans Health Administration, Office of Research and Development, Biomedical Laboratory Research and Development) Grant 1 I01 BX000972-01A1, National Cancer Institute Grants CA097274 (University of Iowa/Mayo Clinic Lymphoma Specialized Program of Research Excellence) and P30CA086862 (Core Support), and the University of Iowa Carver College of Medicine Carver Medical Research Initiative Grant to C.T.M. The content of this manuscript are solely the responsibility of the authors and do not necessarily represent the official views of the granting agencies.

Abbreviations used in this article

BTN	butyrophilin
HMBcPP	(*E*)-1-hydroxy-2-methyl-pent-2-enyl pyrophosphonate
HMBPP	(*E*)-4-hydroxy-3-methyl-but-2-enyl pyrophosphate (diphosphate)
IgC	immunoglobulin C-like
IgV	immunoglobulin V-like
IPP	isopentenyl pyrophosphate (diphosphate)
MFI	mean fluorescence intensity
siRNA	small interfering RNA
TRIM	tripartite motif-containing

References

1. Morita CT, Jin C, Sarikonda G, Wang H. Nonpeptide antigens, presentation mechanisms, and immunological memory of human Vγ2Vδ2 T cells: discriminating friend from foe through the recognition of prenyl pyrophosphate antigens. Immunol. Rev. 2007; 215:59–76. [PubMed: 17291279]
2. Bukowski JF, Morita CT, Tanaka Y, Bloom BR, Brenner MB, Band H. Vγ2Vδ2 TCR-dependent recognition of non-peptide antigens and Daudi cells analyzed by TCR gene transfer. J. Immunol. 1995; 154:998–1006. [PubMed: 7529807]
3. Puan K-J, Jin C, Wang H, Sarikonda G, Raker AM, Lee HK, Samuelson MI, Märker-Hermann E, Pasa-Tolic L, Nieves E, Giner J-L, Kuzuyama T, Morita CT. Preferential recognition of a microbial metabolite by human Vγ2Vδ2 T cells. Int. Immunol. 2007; 19:657–673. [PubMed: 17446209]
4. Hintz M, Reichenberg A, Altincicek B, Bahr U, Gschwind RM, Kollas A-K, Beck E, Wiesner J, Eberl M, Jomaa H. Identification of (*E*)-4-hydroxy-3-methyl-but-2-enyl pyrophosphate as a major activator for human γδ T cells in *Escherichia coli*. FEBS Lett. 2001; 509:317–322. [PubMed: 11741609]
5. Tanaka Y, Morita CT, Tanaka Y, Nieves E, Brenner MB, Bloom BR. Natural and synthetic non-peptide antigens recognized by human γδ T cells. Nature. 1995; 375:155–158. [PubMed: 7753173]
6. Dieli F, Troye-Blomberg M, Ivanyi J, Fournié JJ, Krensky AM, Bonneville M, Peyrat MA, Caccamo N, Sireci G, Salerno A. Granulysin-dependent killing of intracellular and extracellular *Mycobacterium tuberculosis* by Vγ9/Vδ2 T lymphocytes. J. Infect. Dis. 2001; 184:1082–1085. [PubMed: 11574927]
7. Marischen L, Wesch D, Schröder JM, Wiedow O, Kabelitz D. Human γδ T cells produce the protease inhibitor and antimicrobial peptide elafin. Scand. J. Immunol. 2009; 70:547–552. [PubMed: 19906197]
8. Dudal S, Turriere C, Bessoles S, Fontes P, Sanchez F, Liautard J, Liautard JP, Lafont V. Release of LL-37 by activated human Vγ9Vδ2 T cells: a microbicidal weapon against *Brucella suis*. J. Immunol. 2006; 177:5533–5539. [PubMed: 17015740]
9. Kunzmann V, Bauer E, Wilhelm M. γ/δ T-cell stimulation by pamidronate. N. Engl. J. Med. 1999; 340:737–738. [PubMed: 10068336]

10. Bukowski JF, Morita CT, Brenner MB. Human γδ T cells recognize alkylamines derived from microbes, edible plants, and tea: implications for innate immunity. Immunity. 1999; 11:57–65. [PubMed: 10435579]
11. Gober H-J, Kistowska M, Angman L, Jenö P, Mori L, De Libero G. Human T cell receptor γδ cells recognize endogenous mevalonate metabolites in tumor cells. J. Exp. Med. 2003; 197:163–168. [PubMed: 12538656]
12. Thompson K, Rojas-Navea J, Rogers MJ. Alkylamines cause Vγ9Vδ2 T-cell activation and proliferation by inhibiting the mevalonate pathway. Blood. 2006; 107:651–654. [PubMed: 16179378]
13. Wang H, Sarikonda G, Puan K-J, Tanaka Y, Feng J, Giner J-L, Cao R, Mönkkönen J, Oldfield E, Morita CT. Indirect stimulation of human Vγ2Vδ2 T cells through alterations in isoprenoid metabolism. J. Immunol. 2011; 187:5099–5113. [PubMed: 22013129]
14. Wilhelm M, Kunzmann V, Eckstein S, Reimer P, Weissinger F, Ruediger T, Tony H-P. γδ T cells for immune therapy of patients with lymphoid malignancies. Blood. 2003; 102:200–206. [PubMed: 12623838]
15. Dieli F, Vermijlen D, Fulfaro F, Caccamo N, Meraviglia S, Cicero G, Roberts A, Buccheri S, D'Asaro M, Gebbia N, Salerno A, Eberl M, Hayday AC. Targeting human γδ T cells with zoledronate and interleukin-2 for immunotherapy of hormone-refractory prostate cancer. Cancer Res. 2007; 67:7450–7457. [PubMed: 17671215]
16. Sakamoto M, Nakajima J, Murakawa T, Fukami T, Yoshida Y, Murayama T, Takamoto S, Matsushita H, Kakimi K. Adoptive immunotherapy for advanced non-small cell lung cancer using zoledronate-expanded γδ T cells: a phase I clinical study. J Immunother. 2011; 34:202–211. [PubMed: 21304399]
17. Kobayashi H, Tanaka Y, Shimmura H, Minato N, Tanabe K. Complete remission of lung metastasis following adoptive immunotherapy using activated autologous γδ T-cells in a patient with renal cell carcinoma. Anticancer Res. 2010; 30:575–579. [PubMed: 20332473]
18. Kobayashi H, Tanaka Y, Yagi J, Minato N, Tanabe K. Phase I/II study of adoptive transfer of γδ T cells in combination with zoledronic acid and IL-2 to patients with advanced renal cell carcinoma. Cancer Immunol. Immunother. 2011; 60:1075–1084. [PubMed: 21519826]
19. Nicol AJ, Tokuyama H, Mattarollo SR, Hagi T, Suzuki K, Yokokawa K, Nieda M. Clinical evaluation of autologous *gamma delta* T cell-based immunotherapy for metastatic solid tumours. Br. J. Cancer. 2011; 105:778–786. [PubMed: 21847128]
20. Palakodeti A, Sandstrom A, Sundaresan L, Harly C, Nedellec S, Olive D, Scotet E, Bonneville M, Adams EJ. The molecular basis for modulation of human Vγ9Vδ2 T cell responses by CD277/butyrophilin-3 (BTN3A)-specific antibodies. J. Biol. Chem. 2012; 287:32780–32790. [PubMed: 22846996]
21. Harly C, Guillaume Y, Nedellec S, Peigné C-M, Mönkkönen H, Mönkkönen J, Li J, Kuball J, Adams EJ, Netzer S, Déchanet-Merville J, Léger A, Herrmann T, Breathnach R, Olive D, Bonneville M, Scotet E. Key implication of CD277/butyrophilin-3 (BTN3A) in cellular stress sensing by a major human γδ T-cell subset. Blood. 2012; 120:2269–2279. [PubMed: 22767497]
22. Wang H, Henry O, Distefano MD, Wang YC, Räikkönen J, Mönkkönen J, Tanaka Y, Morita CT. Butyrophilin 3A1 plays an essential role in prenyl pyrophosphate stimulation of human Vγ2Vδ2 T cells. J. Immunol. 2013; 191:1029–1042. [PubMed: 23833237]
23. Vavassori S, Kumar A, Wan GS, Ramanjaneyulu GS, Cavallari M, El Daker S, Beddoe T, Theodossis A, Williams NK, Gostick E, Price DA, Soudamini DU, Voon KK, Olivo M, Rossjohn J, Mori L, De Libero G. Butyrophilin 3A1 binds phosphorylated antigens and stimulates human γδ T cells. Nat. Immunol. 2013; 14:908–916. [PubMed: 23872678]
24. Esser C. A fat story-antigen presentation by butyrophilin 3A1 to γδ T cells. Cell. Mol. Immunol. 2014; 11:5–7. [PubMed: 24097036]
25. Sandstrom A, Peigné C-M, Léger A, Crooks JE, Konczak F, Gesnel M-C, Breathnach R, Bonneville M, Scotet E, Adams EJ. The intracellular B30.2 domain of butyrophilin 3A1 binds phosphoantigens to mediate activation of human Vγ9Vδ2 T cells. Immunity. 2014; 40:490–500. [PubMed: 24703779]

26. Hsiao C-HC, Lin X, Barney RJ, Shippy RR, Li J, Vinogradova O, Wiemer DF, Wiemer AJ. Synthesis of a phosphoantigen prodrug that potently activates Vγ9Vδ2 T-lymphocytes. Chem. Biol. 2014; 21:945–954. [PubMed: 25065532]
27. Rhodes DA, Chen HC, Price AJ, Keeble AH, Davey MS, James LC, Eberl M, Trowsdale J. Activation of human γδ T cells by cytosolic interactions of BTN3A1 with soluble phosphoantigens and the cytoskeletal adaptor periplakin. J. Immunol. 2015; 194:2390–2398. [PubMed: 25637025]
28. Riaño F, Karunakaran MM, Starick L, Li J, Scholz CJ, Kunzmann V, Olive D, Amslinger S, Herrmann T. Vγ9Vδ2 TCR-activation by phosphorylated antigens requires butyrophilin 3 A1 (*BTN3A1*) and additional genes on human chromosome 6. Eur. J. Immunol. 2014; 44:2571–2576. [PubMed: 24890657]
29. Delorenzi M, Speed T. An HMM model for coiled-coil domains and a comparison with PSSM-based predictions. Bioinformatics. 2002; 18:617–625. [PubMed: 12016059]
30. Wood CW, Bruning M, Ibarra AÁ, Bartlett GJ, Thomson AR, Sessions RB, Brady RL, Woolfson DN. CCBuilder: an interactive web-based tool for building, designing and assessing coiled-coil protein assemblies. Bioinformatics. 2014; 30:3029–3035. [PubMed: 25064570]
31. Call ME, Wucherpfennig KW, Chou JJ. The structural basis for intramembrane assembly of an activating immunoreceptor complex. Nat. Immunol. 2010; 11:1023–1029. [PubMed: 20890284]
32. Baker NA, Sept D, Joseph S, Holst MJ, McCammon JA. Electrostatics of nanosystems: application to microtubules and the ribosome. Proc. Natl. Acad. Sci. USA. 2001; 98:10037–10041. [PubMed: 11517324]
33. Willcox CR, Mohammed F, Willcox BE. Resolving the mystery of pyrophosphate antigen presentation. Nat. Immunol. 2013; 14:886–887. [PubMed: 23959177]
34. Woo J-S, Suh H-Y, Park S-Y, Oh B-H. Structural basis for protein recognition by B30.2/SPRY domains. Mol. Cell. 2006; 24:967–976. [PubMed: 17189197]
35. James LC, Keeble AH, Khan Z, Rhodes DA, Trowsdale J. Structural basis for PRYSPRY-mediated tripartite motif (TRIM) protein function. Proc. Natl. Acad. Sci. USA. 2007; 104:6200–6205. [PubMed: 17400754]
36. Filippakopoulos P, Low A, Sharpe TD, Uppenberg J, Yao S, Kuang Z, Savitsky P, Lewis RS, Nicholson SE, Norton RS, Bullock AN. Structural basis for Par-4 recognition by the SPRY domain- and SOCS box-containing proteins SPSB1, SPSB2, and SPSB4. J. Mol. Biol. 2010; 401:389–402. [PubMed: 20561531]
37. D'Cruz AA, Kershaw NJ, Chiang JJ, Wang MK, Nicola NA, Babon JJ, Gack MU, Nicholson SE. Crystal structure of the TRIM25 B30.2 (PRYSPRY) domain: a key component of antiviral signalling. Biochem. J. 2013; 456:231–240. [PubMed: 24015671]
38. Weinert C, Grütter C, Roschitzki-Voser H, Mittl PR, Grütter MG. The crystal structure of human pyrin B30.2 domain: implications for mutations associated with familial Mediterranean fever. J. Mol. Biol. 2009; 394:226–236. [PubMed: 19729025]
39. Biris N, Yang Y, Taylor AB, Tomashevski A, Guo M, Hart PJ, Diaz-Griffero F, Ivanov DN. Structure of the rhesus monkey TRIM5α PRYSPRY domain, the HIV capsid recognition module. Proc. Natl. Acad. Sci. USA. 2012; 109:13278–13283. [PubMed: 22847415]
40. Rhodes DA, de Bono B, Trowsdale J. Relationship between SPRY and B30.2 protein domains. Evolution of a component of immune defence? Immunology. 2005; 116:411–417. [PubMed: 16313355]
41. Perfetto L, Gherardini PF, Davey NE, Diella F, Helmer-Citterich M, Cesareni G. Exploring the diversity of SPRY/B30.2-mediated interactions. Trends Biochem. Sci. 2013; 38:38–46. [PubMed: 23164942]
42. D'Cruz AA, Babon JJ, Norton RS, Nicola NA, Nicholson SE. Structure and function of the SPRY/B30.2 domain proteins involved in innate immunity. Protein Sci. 2013; 22:1–10. [PubMed: 23139046]
43. Versteeg GA, Rajsbaum R, Sánchez-Aparicio MT, Maestre AM, Valdiviezo J, Shi M, Inn K-S, Fernandez-Sesma A, Jung J, García-Sastre A. The E3-ligase TRIM family of proteins regulates signaling pathways triggered by innate immune pattern-recognition receptors. Immunity. 2013; 38:384–398. [PubMed: 23438823]

44. Versteeg GA, Benke S, García-Sastre A, Rajsbaum R. InTRIMsic immunity: Positive and negative regulation of immune signaling by tripartite motif proteins. Cytokine Growth Factor Rev. 2014; 25:563–576. [PubMed: 25172371]
45. Woo JS, Imm JH, Min CK, Kim KJ, Cha SS, Oh BH. Structural and functional insights into the B30.2/SPRY domain. EMBO J. 2006; 25:1353–1363. [PubMed: 16498413]
46. Tanaka Y, Sano S, Nieves E, De Libero G, Roca D, Modlin RL, Brenner MB, Bloom BR, Morita CT. Nonpeptide ligands for human γδ T cells. Proc. Natl. Acad. Sci. USA. 1994; 91:8175–8179. [PubMed: 8058775]
47. García VE, Jullien D, Song M, Uyemura K, Shuai K, Morita CT, Modlin RL. IL-15 enhances the response of human γδ T cell responses to nonpeptide microbial antigens. J. Immunol. 1998; 160:4322–4329. [PubMed: 9574535]
48. Spada FM, Grant EP, Peters PJ, Sugita M, Melián A, Leslie DS, Lee HK, van Donselaar E, Hanson DA, Krensky AM, Majdic O, Porcelli SA, Morita CT, Brenner MB. Self-recognition of CD1 by γ/δ T cells: implications for innate immunity. J. Exp. Med. 2000; 191:937–948. [PubMed: 10727456]
49. Morita CT, Lee HK, Wang H, Li H, Mariuzza RA, Tanaka Y. Structural features of nonpeptide prenyl pyrophosphates that determine their antigenicity for human γδ T cells. J. Immunol. 2001; 167:36–41. [PubMed: 11418629]
50. Morita CT, Li H, Lamphear JG, Rich RR, Fraser JD, Mariuzza RA, Lee HK. Superantigen recognition by γδ T cells: SEA recognition site for human Vγ2 T cell receptors. Immunity. 2001; 14:331–344. [PubMed: 11290341]
51. Wang H, Lee HK, Bukowski JF, Li H, Mariuzza RA, Chen ZW, Nam K-H, Morita CT. Conservation of nonpeptide antigen recognition by rhesus monkey Vγ2Vδ2 T cells. J. Immunol. 2003; 170:3696–3706. [PubMed: 12646635]
52. Song Y, Zhang Y, Wang H, Raker AM, Sanders JM, Broderick E, Clark A, Morita CT, Oldfield E. Synthesis of chiral phosphoantigens and their activity in γδ T cell stimulation. Bioorg. Med. Chem. Lett. 2004; 14:4471–4477. [PubMed: 15357974]
53. Puan K-J, Wang H, Dairi T, Kuzuyama T, Morita CT. *fldA* is an essential gene required in the 2-*C*-methyl-D-erythritol 4-phosphate pathway for isoprenoid biosynthesis. FEBS Lett. 2005; 579:3802–3806. [PubMed: 15978585]
54. Zhang Y, Y. S, Yin F, Broderick E, Siegel K, Goddard A, Nieves E, Pasa-Tolic L, Tanaka Y, Wang H, Morita CT, Oldfield E. Structural studies of Vγ2Vδ2 T cell phosphoantigens. Chem. Biol. 2006; 13:985–992. [PubMed: 16984888]
55. Tanaka Y, Kobayashi H, Terasaki T, Toma H, Aruga A, Uchiyama T, Mizutani K, Mikami B, Morita CT, Minato N. Synthesis of pyrophosphate-containing compounds that stimulate Vγ2Vδ2 T cells: application to cancer immunotherapy. Med. Chem. 2007; 3:85–99. [PubMed: 17266628]
56. Sarikonda G, Wang H, Puan K-J, Liu X-H, Lee HK, Song Y, Distefano MD, Oldfield E, Prestwich GD, Morita CT. Photoaffinity antigens for human γδ T cells. J. Immunol. 2008; 181:7738–7750. [PubMed: 19017963]
57. Giner J-L, Wang H, Morita CT. Synthesis and immunological evaluation of the 4-β-glucoside of HMBPP. Bioorg. Med. Chem. Lett. 2012; 22:811–813. [PubMed: 22222033]
58. Workalemahu G, Wang H, Puan K-J, Nada MH, Kuzuyama T, Jones BD, Jin C, Morita CT. Metabolic engineering of *Salmonella* vaccine bacteria to boost human Vγ2Vδ2 T cell immunity. J. Immunol. 2014; 193:708–721. [PubMed: 24943221]
59. Kato Y, Tanaka Y, Miyagawa F, Yamashita S, Minato N. Targeting of tumor cells for human γδ T cells by nonpeptide antigens. J. Immunol. 2001; 167:5092–5098. [PubMed: 11673519]
60. Miyagawa F, Tanaka Y, Yamashita S, Minato N. Essential requirement of antigen presentation by monocyte lineage cells for the activation of primary human γδ T cells by aminobisphosphonate antigen. J. Immunol. 2001; 166:5508–5514. [PubMed: 11313389]
61. Murayama M, Tanaka Y, Yagi J, Uchiyama T, Ogawa K. Antitumor activity and some immunological properties of γδ T-cells from patients with gastrointestinal carcinomas. Anticancer Res. 2008; 28:2921–2931. [PubMed: 19031935]
62. Wang H, Fang Z, Morita CT. Vγ2Vδ2 T cell receptor recognition of prenyl pyrophosphates is dependent on all CDRs. J. Immunol. 2010; 184:6209–6222. [PubMed: 20483784]

63. Hebbeler AM, Cairo C, Cummings JS, Pauza CD. Individual Vγ2-Jγ1.2^{+} T cells respond to both isopentenyl pyrophosphate and Daudi cell stimulation: generating tumor effectors with low molecular weight phosphoantigens. Cancer Immunol. Immunother. 2007; 56:819–829. [PubMed: 17131122]
64. Evans PS, Enders PJ, Yin C, Ruckwardt TJ, Malkovsky M, Pauza CD. *In vitro* stimulation with a non-peptidic alkylphosphate expands cells expressing Vγ2-Jγ1.2/Vδ2 T-cell receptors. Immunology. 2001; 104:19–27. [PubMed: 11576216]
65. Davodeau F, Peyrat MA, Hallet MM, Houde I, Vie H, Bonneville M. Peripheral selection of antigen receptor junctional features in a major human γδ subset. Eur. J. Immunol. 1993; 23:804–808. [PubMed: 8384559]
66. Davodeau F, Peyrat M-A, Hallet M-M, Gaschet J, Houde I, Vivien R, Vie H, Bonneville M. Close correlation between Daudi and mycobacterial antigen recognition by human γδ T cells and expression of V9JPC1γ/V2DJCδ-encoded T cell receptors. J. Immunol. 1993; 151:1214–1223. [PubMed: 8393042]
67. Martini F, Paglia MG, Montesano C, Enders PJ, Gentile M, Pauza CD, Gioia C, Colizzi V, Narciso P, Pucillo LP, Poccia F. Vγ9Vδ2 T-cell anergy and complementarity-determining region 3-specific depletion during paroxysm of nonendemic malaria infection. Infect. Immun. 2003; 71:2945–2949. [PubMed: 12704176]
68. Bukowski JF, Morita CT, Band H, Brenner MB. Crucial role of TCRγ chain junctional region in prenyl pyrophosphate antigen recognition by γδ T cells. J. Immunol. 1998; 161:286–293. [PubMed: 9647235]
69. Favier B, Espinosa E, Tabiasco J, Dos Santos C, Bonneville M, Valitutti S, Fournié J-J. Uncoupling between immunological synapse formation and functional outcome in human γδ T lymphocytes. J. Immunol. 2003; 171:5027–5033. [PubMed: 14607899]
70. Grakoui A, Bromley SK, Sumen C, Davis MM, Shaw AS, Allen PM, Dustin ML. The immunological synapse: a molecular machine controlling T cell activation. Science. 1999; 285:221–227. [PubMed: 10398592]
71. Lee KH, Holdorf AD, Dustin ML, Chan AC, Allen PM, Shaw AS. T cell receptor signaling precedes immunological synapse formation. Science. 2002; 295:1539–1542. [PubMed: 11859198]
72. Purtic B, Pitcher LA, van Oers NS, Wülfing C. T cell receptor (TCR) clustering in the immunological synapse integrates TCR and costimulatory signaling in selected T cells. Proc. Natl. Acad. Sci. USA. 2005; 102:2904–2909. [PubMed: 15703298]
73. Diensthuber RP, Bommer M, Gleichmann T, Möglich A. Full-length structure of a sensor histidine kinase pinpoints coaxial coiled coils as signal transducers and modulators. Structure. 2013; 21:1127–1136. [PubMed: 23746806]
74. Boyden LM, Lewis JM, Barbee SD, Bas A, Girardi M, Hayday AC, Tigelaar RE, Lifton RP. Skint1, the prototype of a newly identified immunoglobulin superfamily gene cluster, positively selects epidermal γδ T cells. Nat. Genet. 2008; 40:656–662. [PubMed: 18408721]
75. Barbee SD, Woodward MJ, Turchinovich G, Mention J-J, Lewis JM, Boyden LM, Lifton RP, Tigelaar R, Hayday AC. Skint-1 is a highly specific, unique selecting component for epidermal T cells. Proc. Natl. Acad. Sci. USA. 2011; 108:3330–3335. [PubMed: 21300860]

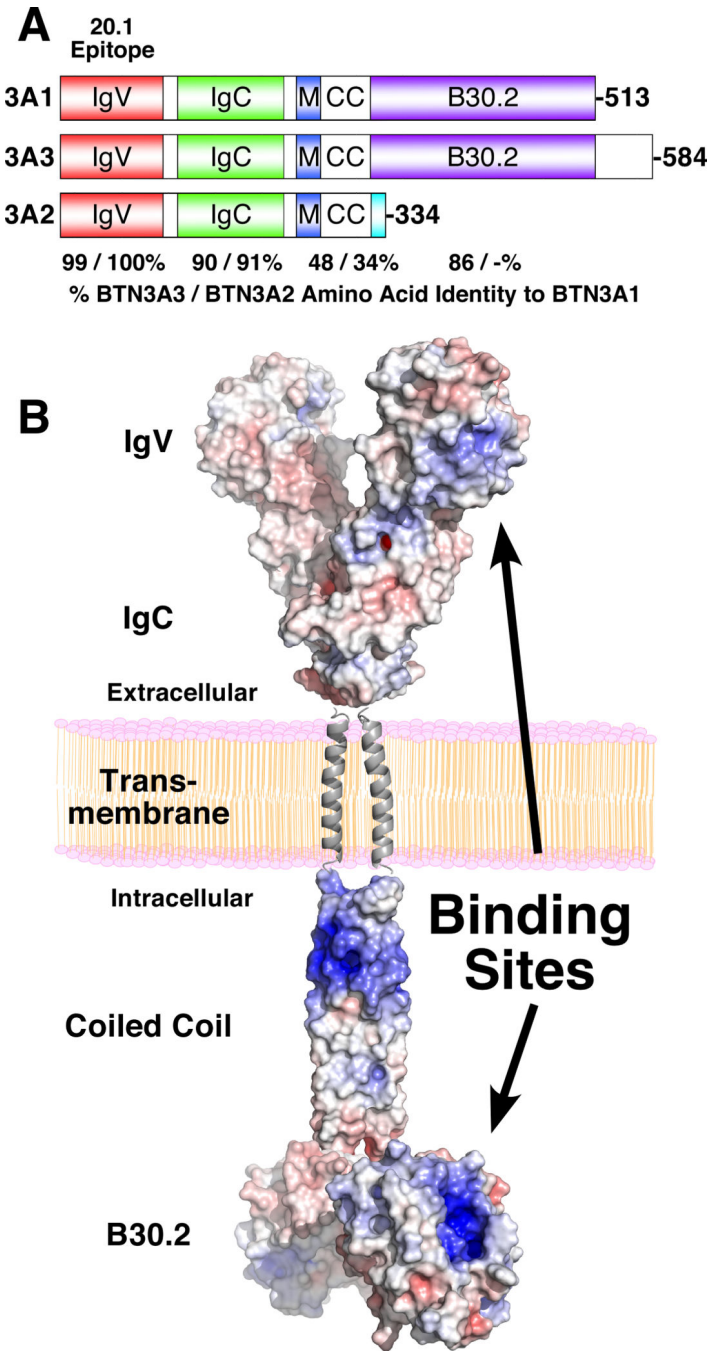

FIGURE 1.

Structural model of BTN3A1 and a schematic of its domain structure. (**A**) Schematic of the domain structure of BTN3A1 in comparison to its two other family members: BTN3A2 and BTN3A3. The stimulatory 20.1 mAb binds to the IgV domain. The percentage of amino acid identity of BTN3A3 and BTN3A2 with BTN3A1 is shown. (**B**) Structural model of BTN3A1 showing the crystal structure of the IgV:IgC extracellular dimer and the B30.2 intracellular dimer and a model of the coiled coil domain. The extracellular dimer is the unbound form. The transmembrane domain is from the DAP12 homodimer.

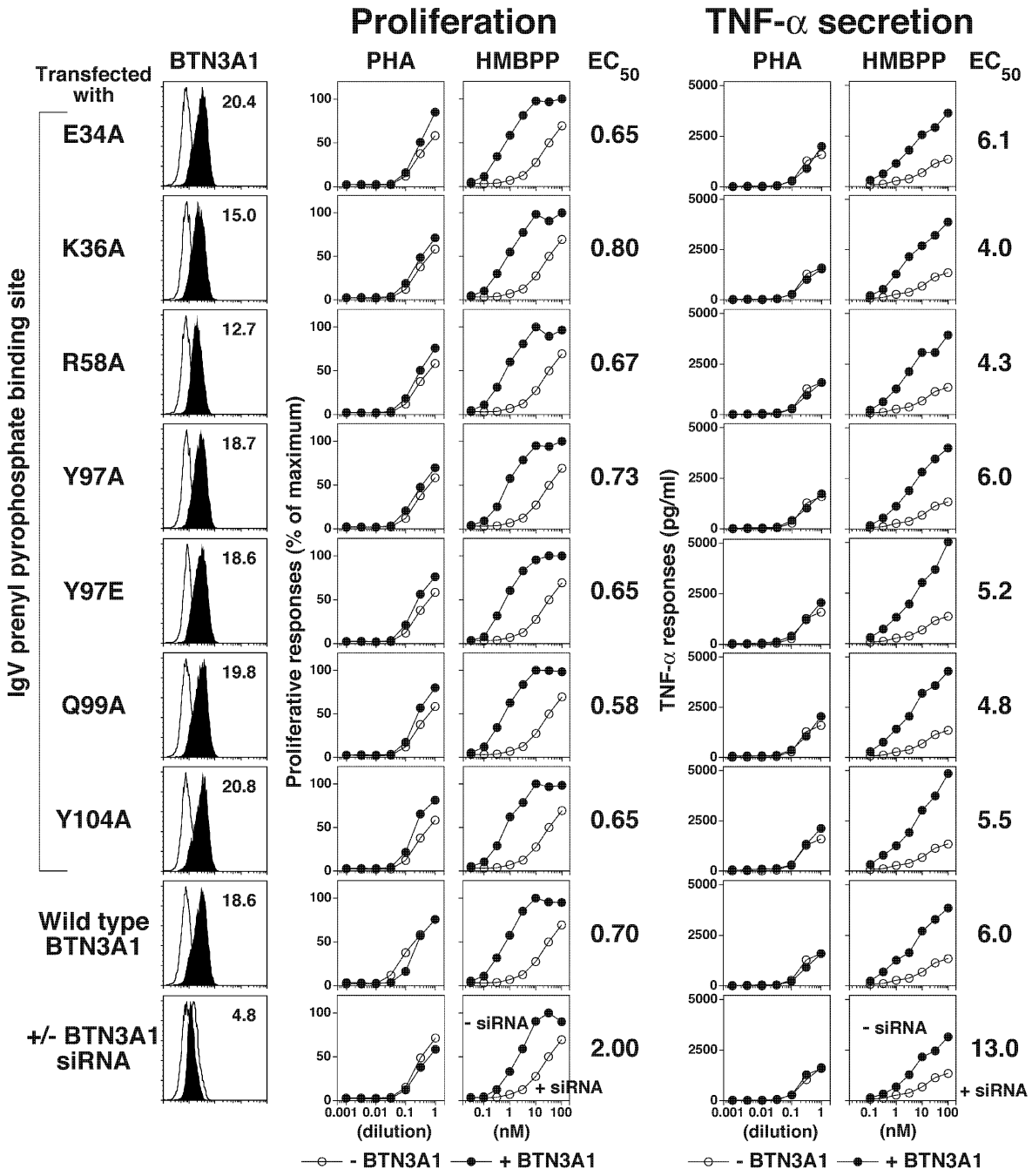

FIGURE 2.

Mutation of residues in the extracellular BTN3A1 IgV binding site have no effect on prenyl pyrophosphate stimulation of Vγ2Vδ2 T cells. BTN3 expression by siRNA-treated HeLa cells expressing mutant or wild type BTN3A1 (*left panels*). Effect of mutations in BTN3A1 on proliferation (*middle panels*) and TNF-α secretion (*right panels*) by Vγ2Vδ2 T cells in response to PHA or HMBPP. Residues in the IgV binding site of BTN3A1 were mutated to alanine or glutamic acid by site-directed mutagenesis. HeLa cells were transfected with a control siRNA, an siRNA specific for the 3'UT region of endogenous BTN3A1 or

cotransfected with an siRNA specific for the 3'UT region of endogenous BTN3A1 and either a wild type or mutated BTN3A1 cDNA. After 72 h, the transfectants were harvested and a portion stained with either PE-P3 IgG1 control mAb or PE-20.1 mAb and analyzed by flow cytometry (*left panels*). The relative mean fluorescence intensity (MFI) was calculated as 20.1 mAb MFI minus isotype control mAb MFI (shown on panels). The remaining cells were treated with mitomycin C and then cultured with 12G12 Vγ2Vδ2 T cells and the PHA mitogen or HMBPP. After 24 h, the supernatants were harvested and TNF-α levels determined by ELISA. The cells were pulsed with [^{3}H]-thymidine and harvested 18 h later. Because of differences in their plateau values, proliferative responses were normalized to set the HMBPP plateau values as 100%. The maximum proliferation values varied for the different HeLa transfectants between 9,200 to 15,444 c.p.m. The EC_{50} values are shown on the right. Representative of two experiments.

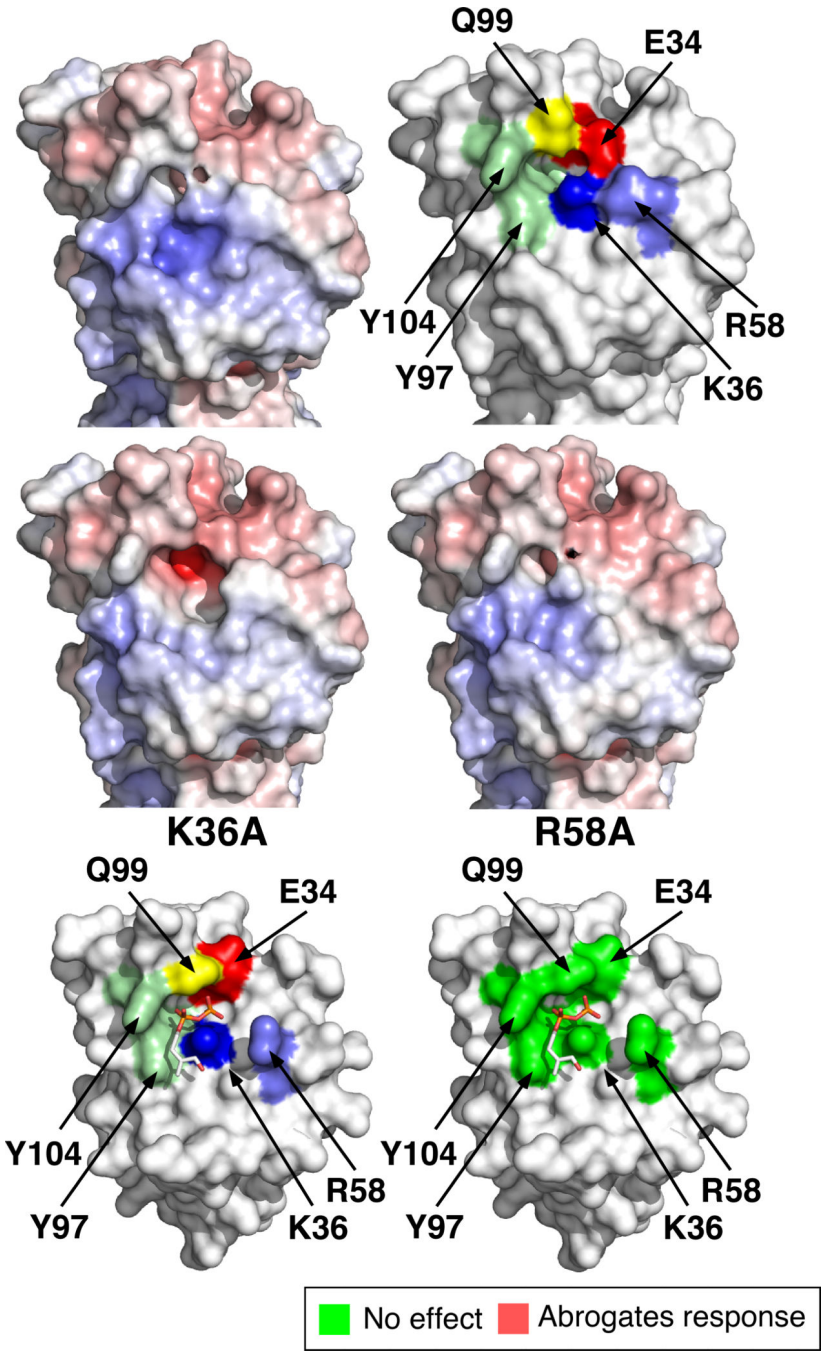

FIGURE 3.

Location and effect of mutated residues in the IgV binding site for prenyl pyrophosphates in BTN3A1 on the stimulation of Vγ2Vδ2 T cells. Surface potential of the IgV binding site (*top left panel*). Surface potentials are colored from red (negative potential, −10 kT) to blue (positive potential, +10 kT). Location of mutated residues in the extracellular dimer of BTN3A1 (PDB 4F80) (*top right panel*). Numbering starts at residue 31 of BTN3A1. Effect of *in silico* alanine mutation of the basic residue, lysine 36, on the surface potential and shape of the IgV binding site (*middle left panel*). Effect of *in silico* alanine mutation of the

basic residue, arginine 58, on the surface potential and shape of the IgV binding site (*middle right panel*). Basic residues were mutated to alanine in silico using PyMOL (Schrödinger), and the surface potential of the mutated BTN3A1 were calculated using the APBS plugin in PyMOL. Structure of BTN3A1 IgV binding to HMBPP (PDB 4K55) (*bottom left panel*). Mutations in the IgV binding site for prenyl pyrophosphates have no effect on proliferation and TNF-α secretion by Vγ2Vδ2 T cells in response to HMBPP (*bottom right panel*). Mutation of residues colored green had no effect (EC_{50} near or at wild type values). Note that none of the mutated residues affected Vγ2Vδ2 T cell stimulation by HMBPP.

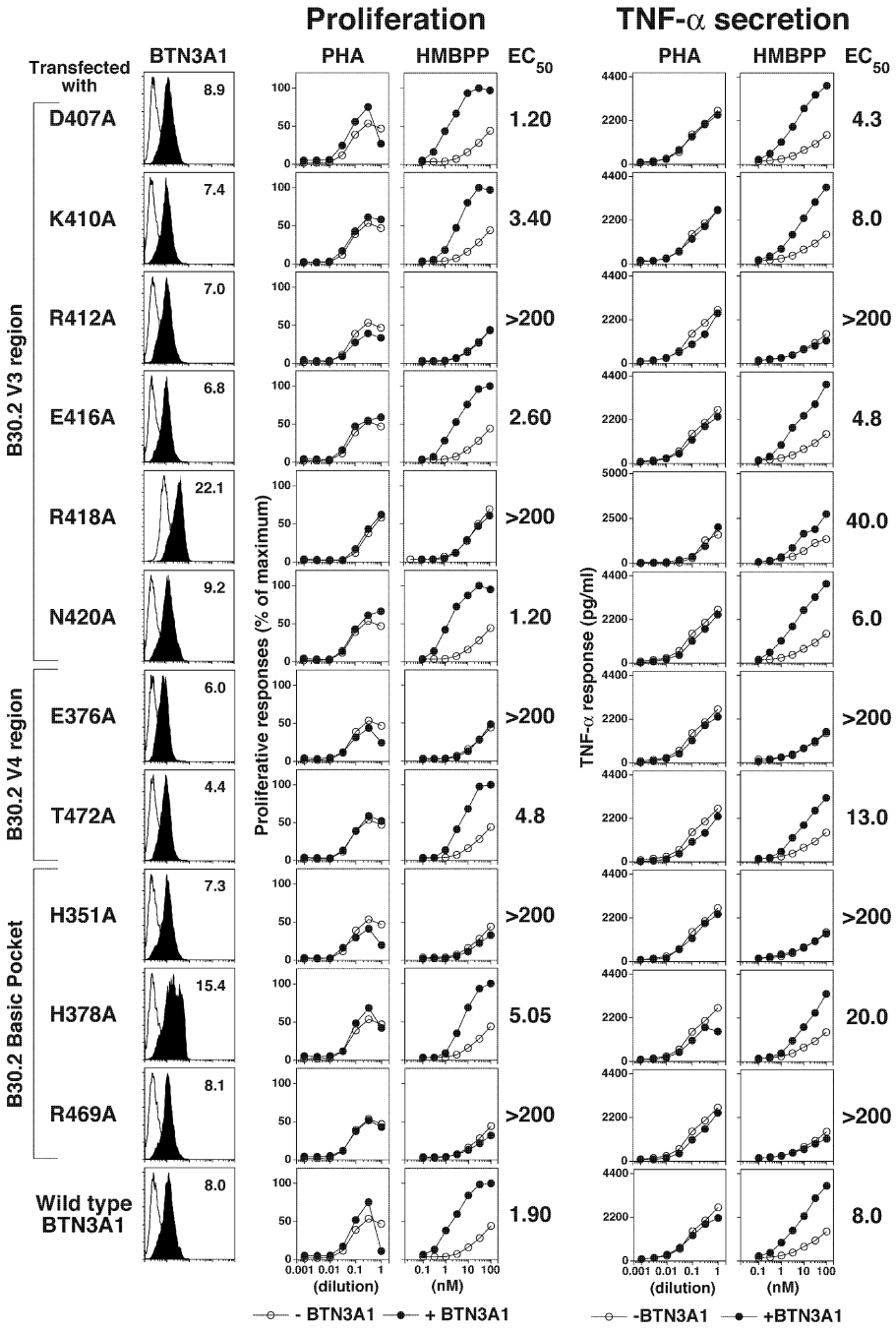

FIGURE 4.

Mutation of residues in the basic pocket and V3 and V4 loops of the B30.2 binding face of BTN3A1 can reduce or abrogate prenyl pyrophosphate stimulation of Vγ2Vδ2 T cells. BTN3 expression by siRNA-treated HeLa cells expressing mutant or wild type BTN3A1 (*left panels*). Effect of mutations in BTN3A1 on proliferation (*middle panels*) and TNF-α secretion (*right panels*) by Vγ2Vδ2 T cells in response to PHA or HMBPP. Residues in the basic pocket and surrounding V3 and V4 regions on the binding face of the B30.2 domain of BTN3A1 were mutated to alanine by site-directed mutagenesis and tested as described in

Fig. 2. Expression of BTN3 was assessed by flow cytometry. Proliferative responses and TNF-α secretion by 12G12 Vγ2Vδ2 T cells in response to the PHA mitogen or HMBPP presented by HeLa cells treated with BTN3A1 siRNA and transfected with wild-type or mutant BTN3A1 were as in Fig. 2. Because of differences in their plateau values, proliferative responses were normalized to set the HMBPP plateau values as 100%. The maximum proliferation values varied for the different HeLa transfectants between 6,070 to 9,701 c.p.m. In cases where proliferation was reduced by mutation of BTN3A1, responses were normalized based on the HMBPP response of HeLa cells treated with control siRNA. Representative of two experiments.

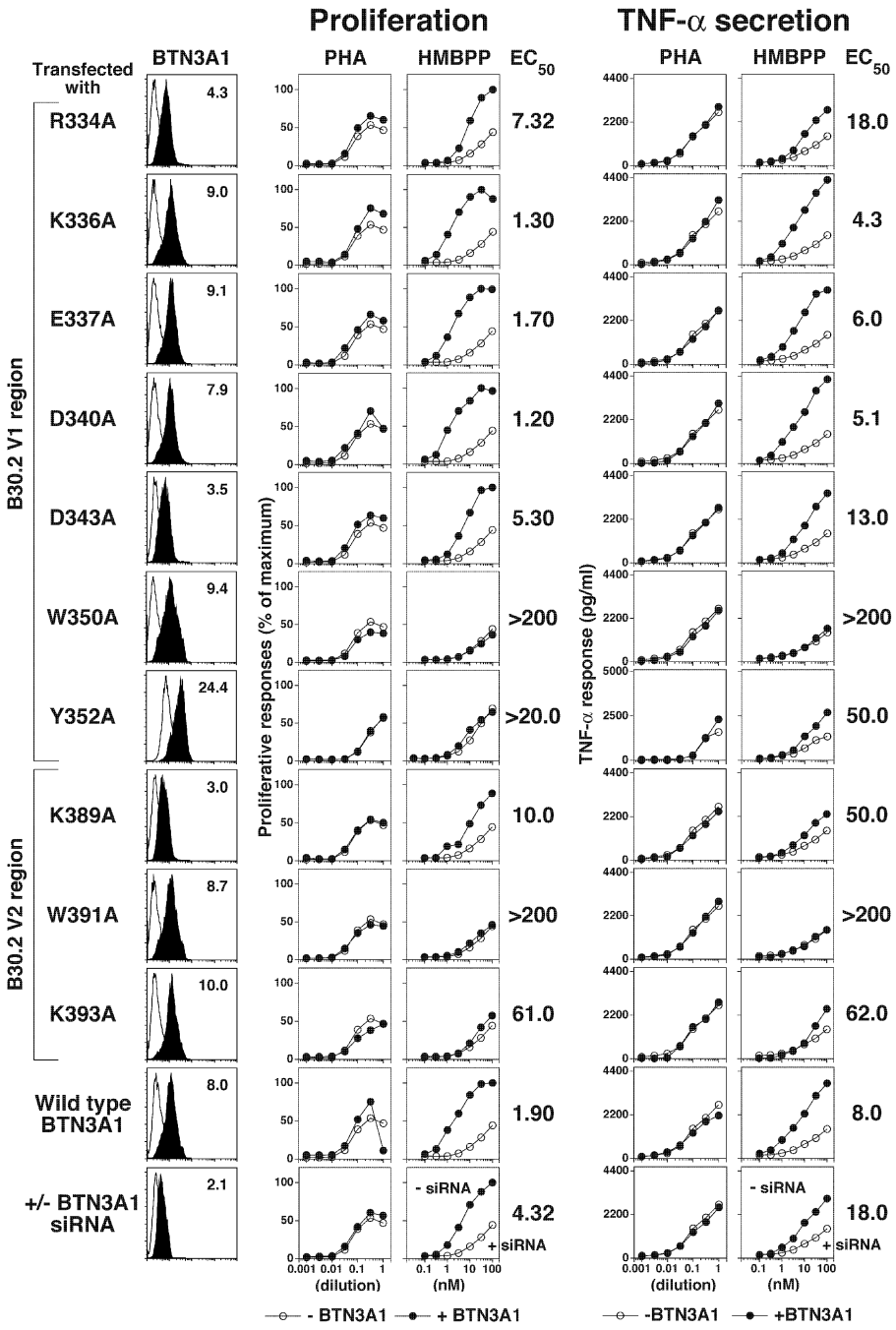

FIGURE 5.

Mutation of residues within the V1 and V2 loops of the B30.2 binding face of BTN3A1 can reduce or abrogate prenyl pyrophosphate stimulation of Vγ2Vδ2 T cells. BTN3 expression by siRNA-treated HeLa cells expressing mutant or wild type BTN3A1 (*left panels*). Effect of mutations in BTN3A1 on proliferation (*middle panels*) and TNF-α secretion (*right panels*) by Vγ2Vδ2 T cells in response to PHA or HMBPP. Residues in the V1 and V2 regions on the binding face of the B30.2 domain of BTN3A1 were mutated to alanine by site-directed mutagenesis and tested as described in Fig. 2. Expression of BTN3 was

assessed by flow cytometry. Proliferative responses and TNF-α secretion by 12G12 Vγ2Vδ2 T cells in response to the PHA mitogen or HMBPP presented by HeLa cells treated with BTN3A1 siRNA and transfected with wild-type or mutant BTN3A1 were as in Fig. 2. Representative of two experiments.

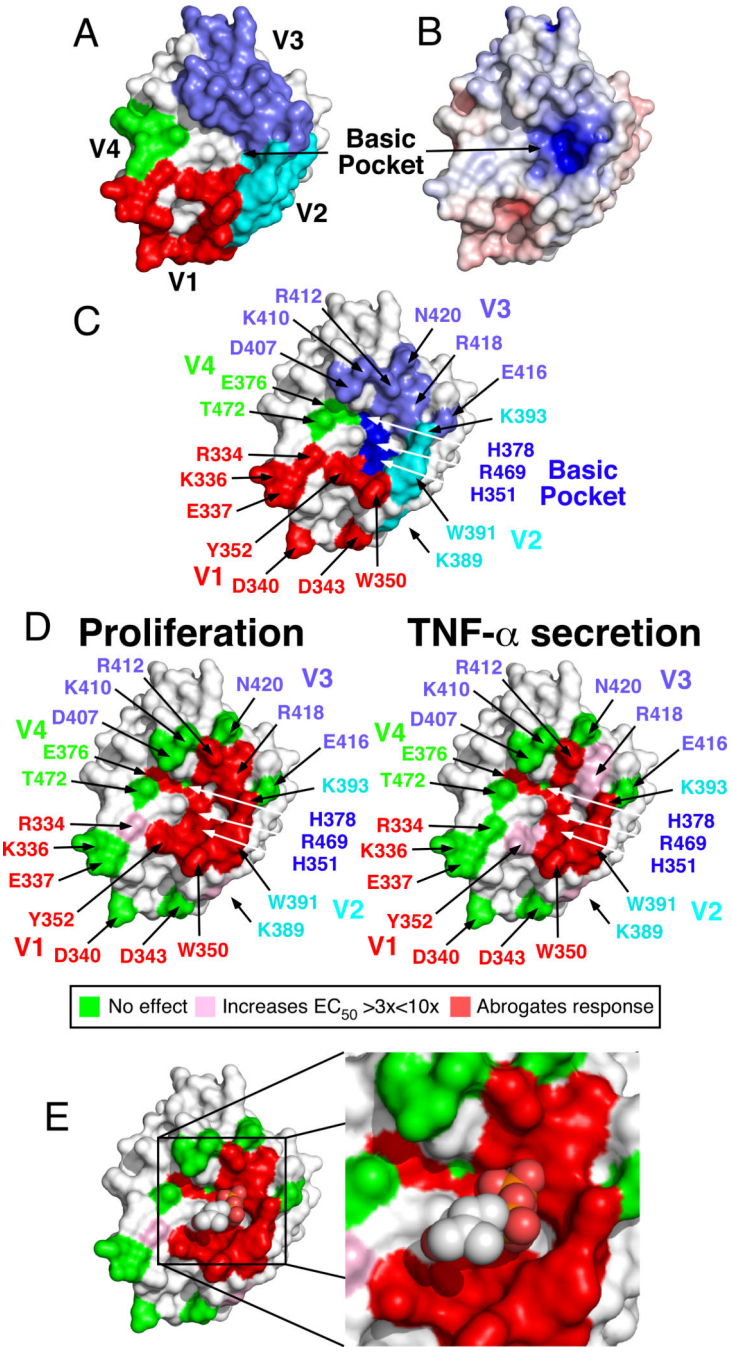

FIGURE 6.

Location and effect of mutated residues in the intracellular B30.2 domain of BTN3A1 on proliferation and TNF-α secretion by Vγ2Vδ2 T cells in response to HMBPP. (**A**) Location of V regions on the binding face of the B30.2 domain of BTN3A1. (**B**) Surface potential of the B30.2 domain of BTN3A1 showing the central basic pocket. Surface potentials are colored from red (negative potential, −10 kT) to blue (positive potential, +10 kT). (**C**) Location of mutated residues in the B30.2 domain. Numbering starts at residue 31 of BTN3A1. (**D**) Location and effect of B30.2 domain mutations on prenyl pyrophosphate

stimulation of Vγ2Vδ2 T cells. Effect of B30.2 domain mutations on proliferation (*left panel*) and TNF-α secretion (*right panel*) by Vγ2Vδ2 T cells stimulated with HMBPP. Mutation of residues colored green had no effect, those colored pink reduced stimulation (EC_{50} 3- to 10-fold greater), and those colored red abrogated stimulation (EC_{50} near or at values observed with siRNA-treated HeLa cells). (**E**) Effects of B30.2 domain mutations on the proliferation of Vγ2Vδ2 T cells shown on the structure of the BTN3A1 B30.2 domain in complex with HMBcPP. The insert shows a close-up view of HMBcPP in complex with the central basic pocket.

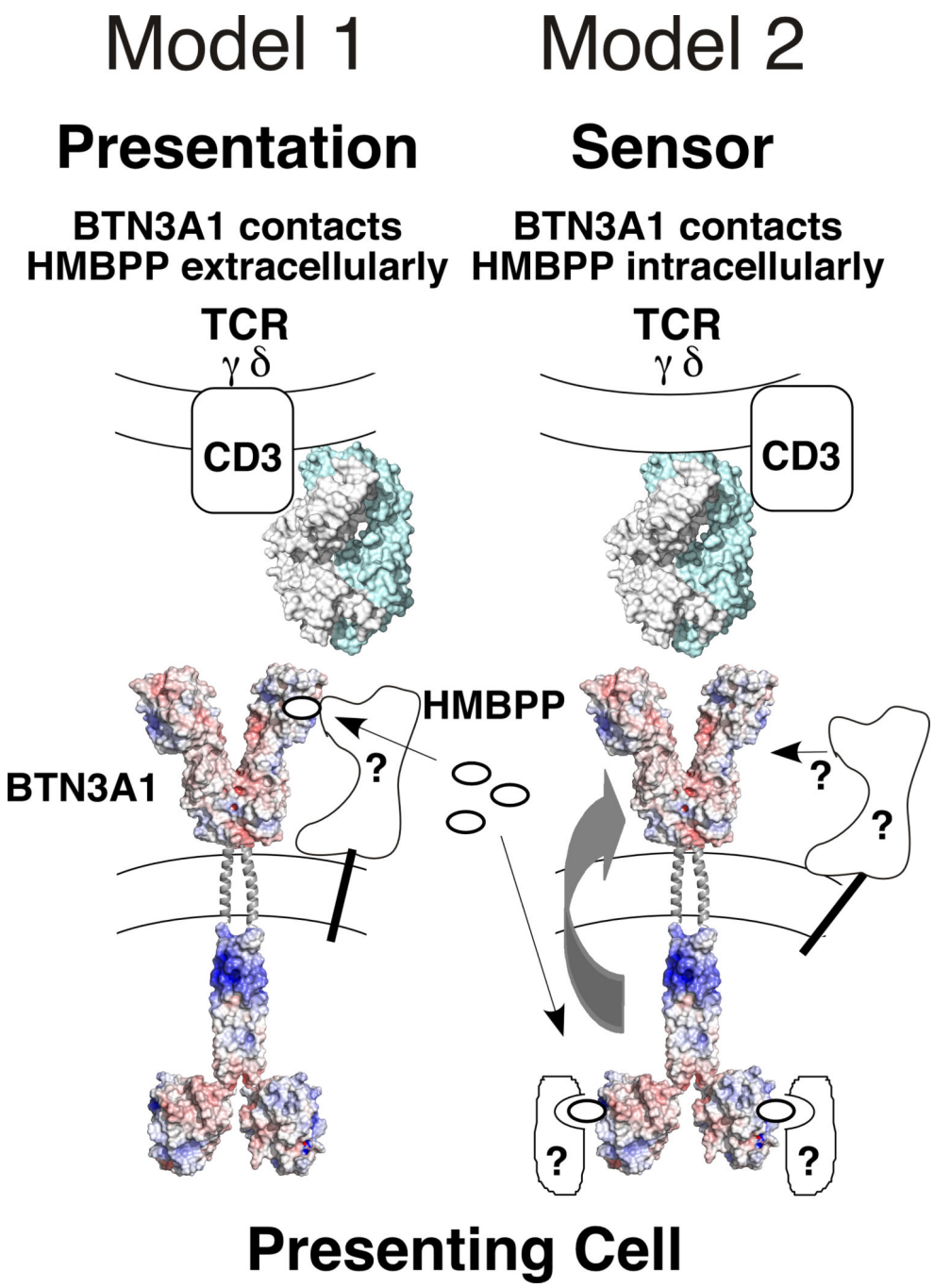

FIGURE 7.

Models for the role of BTN3A1 in prenyl pyrophosphate stimulation of Vγ2Vδ2 T cells. In model 1, BTN3A1 functions as a presenting molecule by binding prenyl pyrophosphates extracellularly with or without the contribution of a second protein. The BTN3A1/prenyl pyrophosphate complex is then directly recognized by the Vγ2Vδ2 TCR. In model 2, BTN3A1 functions as a sensor for intracellular prenyl pyrophosphates and other phosphoantigens. The BTN3A1 B30.2 domain binds prenyl pyrophosphates directly, likely in association with a second protein that enhances or stabilizes binding. This intracellular

binding of prenyl pyrophosphates to the B30.2 domain and association with a second protein results in a change in BTN3A1 conformation and/or distribution leading to Vγ2Vδ2 T cell stimulation through Vγ2Vδ2 TCR recognition of either BTN3A1 in an altered conformation or of another protein recruited to BTN3A1.